Eur. Phys. J. D **12**, 255–261 (2000)

**THE EUROPEAN PHYSICAL JOURNAL D**

EDP Sciences


# Pump probe experiment in atomic fine structure levels: Observation of the oscillation of an angular wavepacket

S. Zamith[a], M.A. Bouchene, E. Sokell[b], C. Nicole[c], V. Blanchet, and B. Girard

Laboratoire de Collisions Agrégats Réactivité[d], IRSAMC, Université Paul Sabatier, 118 route de Narbonne, 31062 Toulouse Cedex 4, France

Received 30 July 1999 and Received in final form 4 April 2000

**Abstract.** Spin precession is investigated through a pump-probe technique which represents an alternative method to previous investigations by wavepacket interferometry. The excited wavepacket corresponds to a precession of spin and orbital angular momentum around the total angular momentum. We discuss and compare two equivalent descriptions of the phenomena, one given in the stationary states and the other in the bright state-dark state formalism. We show that this latter formalism is the most appropriate to describe the dynamics.

**PACS.** 32.80.Qk Coherent control of atomic interactions with photons – 32.80.Rm Multiphoton ionization and excitation to highly excited states (e.g., Rydberg states) – 42.50.Md Optical transient phenomena: quantum beats, photon echo, free-induction decay, dephasings and revivals, optical nutation, and self-induced transparency

## 1 Introduction

With the advent of ultrashort laser pulses, it has become possible to study directly dynamical phenomena in many microscopic systems, from the gas phase to the condensed phase [1–3]. Studies can be arranged in several categories depending on the nature of the phenomena observed. In simple systems, periodic motions can be observed. These dynamics can in general be predicted from the Fourier transform of the absorption lines measured by standard spectroscopy. However, time resolved studies provide a direct insight into the dynamics, with a simple connection to semiclassical interpretations. Among the many systems studied, wavepacket dynamics of nuclear motion in small molecules (vibration [4–12] and dissociation [13–17]) and Rydberg electron dynamics in atoms (angular and radial motion) [18,19] continue to receive much attention [20–22]. Also, the dynamics of spin-orbit precession have been recently reported [23,24].

Fine structure states in alkali atoms have been widely studied using conventional or quantum beat [25] spectroscopy and their structures and wave functions have been well-known for many years [26]. However, in contrast to Rydberg electron wavepackets, very few time-resolved experiments aimed at observing quantum wavepackets in fine structure levels have been attempted [23,24]. In the former case, the semi-classical radial or angular motion associated with the wavepacket has motivated many studies. On the contrary, the spin-orbit precession dynamics has perhaps been largely overlooked. Up to now direct observations of fine structure dynamics in atoms have been performed by using wavepacket interferences that do not require a probe step [23,27,28]. However this technique has experimental constraints: the signal must be sampled with a high time delay resolution, better than the optical period, and this requires long acquisition times. Moreover the beats observed in these experiments do not show unambiguously that a wavepacket is created [28–30]. This technique provides clear evidence for wavepacket creation only when it is implemented in the saturation regime where non-linearities mix the transition frequencies [24, 31,32]. For instance, two separate initial hyperfine structure levels produce the same beat pattern, but without any wavepacket creation [33]. This is also the case for two isotope with neighbouring transitions, as well as for molecules in several initial rovibrational states [34].

In this paper we present a pump probe experiment performed in the fine structure levels of the ($4s$–$4p$) transition in atomic potassium. A time delay dependent signal was experimentally observed. We present a theoretical analysis in two different frameworks, the conventional stationary basis set and the bright-dark states basis. We discuss the conditions that are required in order to observe pump-probe signals in both cases. Even though these representations are equivalent they do not provide the same physical insight. The nature of the corresponding

[a] e-mail: sebas@yosemite.ups-tlse.fr

[b] *Present address*: Physics Dept., University College Dublin, Belfield, Dublin 4, Ireland.

[c] *Present address*: FOM Institute for Atomic and Molecular Physics, Kruislaan 407, 1098 SJ Amsterdam, The Netherlands.

[d] UMR 5589 du CNRS

wavepacket and its dynamics are not intuitively understood using a framework of stationary states. We demonstrate that the bright state-dark state formalism is better adapted to give a simple and direct understanding of the experiment and of the nature of the fine structure wavepacket. This formalism shares many common features with the doorway state-window state picture commonly used in molecular physics to describe transitions towards complex structures in polyatomic molecules [35]. In atomic physics, it has been widely used to describe various phenomena such as dark resonances [36], laser cooling below the one-photon recoil limit [37], Stimulated Rapid Adiabatic Passage (STIRAP) [38,39] and more general coherent phenomena in three level systems [40]. It provides physical insight into these phenomena and an image of the interactions that is not provided by the stationary state description.

## 2 Theory

The pump-probe scheme consists of using a combination of two ultrashort pulses to excite a quantum system and to analyse the degree of evolution after a given time delay between the pulses. The first pulse prepares a wavepacket, which is a quantum superposition of excited states. After free evolution of the wavepacket, the second pulse excites it towards a final state. If this last step depends on the degree of evolution of the system, then the delay dependent final state probability reveals the dynamics of the system. We will show here that such dynamics can be treated using two equivalent formalisms. The formalism of coherently excited stationary states is the most commonly used. Alternatively, when the wavepacket is associated with one coordinate, such as the internuclear distance in a diatomic molecule or the angular or radial coordinates of a Rydberg electron, its evolution can often be described as the semi-classical evolution of a wavepacket. We use here the formalism of bright state-dark states which shares many features with semi-classical wavepacket dynamics. In both cases, the wavepacket is projected onto a basis of non-stationary states built as a superposition of stationary states, with projection coefficients depending on the excitation step.

### 2.1 Description in the stationary basis state

We consider a system with a ground state $|g\rangle$ (taken as the energy origin) and excited states $|k\rangle$ ($k = a, b, c...$) with energies $\omega_k$ and an ionisation continuum $|f\rangle$. The first laser pulse, of duration $\tau_{\rm L}$, centred at time $t = 0$, excites a coherent superposition of the excited states. In the limit of a short pulse, with a spectral width $\Delta\omega_{\rm L}$ that is sufficiently broad to excite all of the intermediate states, the wavepacket in the excited states at time $t \gg \tau_{\rm L}$ is given by

$$|\psi(t)\rangle = \sum_k \mathcal{E}_1(\omega_k)\mu_{kg}\mathrm{e}^{-\mathrm{i}\omega_k t}|k\rangle \qquad (1)$$

where $\mu_{kg}$ represents the matrix element for the $|g\rangle \rightarrow |k\rangle$ transition of the dipole moment operator $\mu$ and $\mathcal{E}_1(\omega_k)$ is the pump pulse laser electric field spectrum at frequency $\omega_k$. The coherent superposition is then probed at a later time $\tau$ by a second ultrashort pulse which ionises the system towards a set of orthogonal continuum states. When the two pulses are well separated ($\tau \gg \tau_{\rm L}$), the probability of excitation of each ion state $|f\rangle$ is given by

$$P_f(\tau) = |\langle f|\mu\mathcal{E}_2(\omega)|\psi(\tau)\rangle|^2 \qquad (2)$$

and the total measured ion signal $P(\tau)$ is the sum over all the final states (if they are orthogonal) $P(\tau) = \sum_f P_f(\tau)$. From relations (1, 2), and in the limit of ultrashort pulses where $\mathcal{E}_1(\omega_{kg}) \cong \mathcal{E}_1(\omega_{1\rm L})$, $\mathcal{E}_2(\omega_{fk}) \cong \mathcal{E}_2(\omega_{2\rm L})$, (where $\omega_{1\rm L}$ and $\omega_{2\rm L}$ are the central laser frequencies) we obtain:

$$P(\tau) = |\mathcal{E}_1(\omega_{1\rm L})|^2|\mathcal{E}_2(\omega_{2\rm L})|^2 \times \sum_{f,k,k'} \mu_{kg}\mu^*_{k'g}\mu_{fk}\mu^*_{fk'}\mathrm{e}^{-\mathrm{i}(\omega_{\rm k}-\omega_{\rm k'})\tau}. \qquad (3)$$

For the $k \neq k'$ contributions, this probability oscillates as a function of the delay time $\tau$ at the relative frequencies $\omega_{kk'} = \omega_k - \omega_{k'}$. These oscillations result from quantum beats between two paths sharing the same initial and final states, and involving the $|k\rangle$ or $|k'\rangle$ state respectively: $|g\rangle \rightarrow |k\rangle \rightarrow |f\rangle$ and $|g\rangle \rightarrow |k'\rangle \rightarrow |f\rangle$. The contrast of these beats is governed by the relative values of the diagonal ($k = k'$) and non-diagonal ($k \neq k'$) dipole moment products $\mu_{kg}\mu^*_{k'g}\mu_{fk}\mu^*_{fk'}$. The pump probe signal reveals the dynamics of the system only if the probe step probability varies significantly with the time delay. There are several reasons why this condition may not be satisfied. The probe step must connect the various excited states to the same final one. The ability to fulfil this condition may be severely constrained by selection rules. The beat contrast is high only if all these transitions are allowed and have comparable strengths and the largest contrast is obtained when the amplitudes of the transitions are equal. In cases where these difficulties can be circumvented the pump-probe method is an efficient method for revealing the dynamics of the excited states. The sign of the dipole moments product fixes the initial phase of the oscillation. In a two state system $|a\rangle$ and $|b\rangle$, only two simple cases can be encountered. If $\mu_{ag}\mu^*_{bg}\mu_{fa}\mu^*_{fb}$ is positive (negative) then the interference is constructive (destructive) for $\tau = 0$ and for each multiple value of the oscillation period the signal is maximal (minimal). In the next section it will be demonstrated how the bright-dark states formalism provides a direct physical meaning for this initial phase.

The stationary state treatment presented above fully describes the observed phenomena. However, it is not always easy to estimate quantitatively or even qualitatively the values of the transition dipole moments and thus to evaluate the phase and amplitude of the oscillations. Another view of the process can be given using the non-stationary states of the bright-dark states framework. This leads to a time dependent description of the interaction process with a more direct physical interpretation.

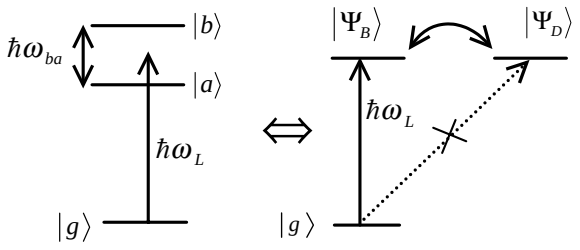


**Fig. 1.** Diagram of the stationary states (left) and bright state-dark state basis sets (right). In the stationary basis set the laser pulse populates both fine structure levels. The temporal evolution is governed by the differences in energies of the system. In the bright-dark state basis set, only the bright state is coupled with the laser field. After the creation of a wavepacket in the bright state the evolution between the bright and dark states is governed by the spin-orbit coupling.

### 2.2 Description in the bright-dark states basis

This description is analogous to the treatment commonly used for vibrational or Rydberg wavepackets. The general definition of the bright state, for $N$ excited states is

$$|\psi_{\mathrm{B}}\rangle = \frac{1}{\sum\limits_{k} |\mu_{kg}|^2} \sum_{k=1}^{N} \mu_{kg} |k\rangle. \tag{4}$$

This corresponds to the projection of the ground state onto the excited state manifold under the action of the electric dipole transition operator. The dark states can be defined freely as any basis set in the subspace orthogonal to the bright state. If the stationary states are non-degenerate, then the bright state and dark states are coupled together by the atomic Hamiltonian. The free evolution results in a transfer of the wavepacket from the bright state to the dark states. Eventually, depending on the size of the manifold and on the energy spacing, the wavepacket comes back (partially or totally) to the bright state during its evolution.

In the case of two excited states, the bright and dark states may be defined respectively by:

$$\begin{aligned} |\psi_{\mathrm{B}}\rangle &= \cos\alpha |a\rangle + \sin\alpha |b\rangle \\ |\psi_{\mathrm{D}}\rangle &= -\sin\alpha |a\rangle + \cos\alpha |b\rangle \end{aligned} \tag{5}$$

where $\tan\alpha = \mu_{bg}/\mu_{ag}$. The laser field couples only the ground and the bright states whilst the atomic Hamiltonian couples the bright and dark states (Fig. 1). When the spectral width of the laser pulse is large compared to $\omega_{ba}$, as is usually the case for an ultrashort pulse, we can separate the laser interaction from the free evolution of the system. The evolution of the system can then be described sequentially. The interaction with the first pulse results in the creation of a wavepacket localised in the bright state. During the short pulse there is no significant leak of population to the dark state. After the pulse ends, the wavepacket evolves freely and may be expressed at time $t$ as:

$$\begin{aligned} |\psi(t)\rangle = \mathrm{e}^{-\mathrm{i}\frac{H}{\hbar}t} |\psi_{\mathrm{B}}\rangle = \mathrm{e}^{-\mathrm{i}\omega_a t}[(\cos^2\alpha + \sin^2\alpha\, \mathrm{e}^{\mathrm{i}\omega_{ba}t})|\psi_{\mathrm{B}}\rangle \\ + \sin\alpha\cos\alpha(-1 + \mathrm{e}^{-\mathrm{i}\omega_{ba}t})|\psi_{\mathrm{D}}\rangle]. \end{aligned} \tag{6}$$

A periodic oscillation between the two states occurs at the frequency $\omega_{ba}$. Although the minimum population in the dark state is zero when $t_{\mathrm{B},p} = p(2\pi/\omega_{ba})$ (where $p$ is an integer), this is not necessarily the case for the bright state whose minimum population, occurring at $t_{\mathrm{D},p} = (2p+1)\pi/\omega_{ba}$, is $\cos 2\alpha$. Evidently this corresponds to a minimum value of zero when $\alpha = \pi/4$ or $\tan\alpha = 1$, which implies that $\mu_{ag} = \mu_{bg}$. In this case the wavepacket is totally transferred to the dark state after half an oscillation period.

These oscillations can be probed by photoionising the excited states involved *via* a probe pulse centred at delay time $\tau$. The total population in the continuum is obtained by summation over the contributions of each final state $|f\rangle$ and is given by

$$\begin{aligned} P &= \sum_f |\langle f|\mu\mathcal{E}_2(\omega)|\psi(\tau)\rangle|^2 \\ &= \left[P_{\mathrm{B}} + \big((P_{\mathrm{D}} - P_{\mathrm{B}})\sin^2 2\alpha - P_{\mathrm{BD}}\sin 4\alpha\big)\left(\frac{1-\cos\omega_{ba}\tau}{2}\right)\right] \end{aligned} \tag{7}$$

where

$$P_{\mathrm{B}} = \sum_f |\langle f|\mu\mathcal{E}_2(\omega)|\psi_{\mathrm{B}}\rangle|^2 \tag{8a}$$

$$P_{\mathrm{D}} = \sum_f |\langle f|\mu\mathcal{E}_2(\omega)|\psi_{\mathrm{D}}\rangle|^2 \tag{8b}$$

$$P_{\mathrm{BD}} = \sum_f \langle f|\mu\mathcal{E}_2(\omega)|\psi_{\mathrm{B}}\rangle\langle\psi_{\mathrm{D}}|\mu\mathcal{E}_2(\omega)|f\rangle \tag{8c}$$

represent the total ionisation probability from the bright and dark states, and $P_{\mathrm{BD}}$ is the interference term corresponding to the possibility of accessing the same final state $|f\rangle$ simultaneously from the bright and dark states. This interference term was assumed to be real in deriving equation (7).

From equation (7) it is clear that a time dependent signal can only be observed if $\sin 2\alpha \neq 0$. Recalling that $\tan\alpha = \mu_{bg}/\mu_{ag}$, $\sin 2\alpha = 0$ corresponds to excitation to a single state, ($|a\rangle$ when $\alpha = 0$ or $|b\rangle$ when $\alpha = \pi/2$) in which case no oscillations will occur. Furthermore it is necessary that either the ionisation probabilities from the bright and dark states are different ($P_{\mathrm{B}} \neq P_{\mathrm{D}}$), or that the interference term is nonvanishing ($P_{\mathrm{BD}} \neq 0$). Due to the limited number of excited states, this time dependence can only be a simple sine function, oscillating at the relative frequency $\omega_{ba}$. Depending on the sign of the quantity $\big((P_{\mathrm{D}} - P_{\mathrm{B}})\sin^2 2\alpha - P_{\mathrm{BD}}\sin 4\alpha\big)$, the oscillation has either a maximum or a minimum at $\tau = 0$. Consequently, the initial phase ($\varphi_0$) can have only two values, 0 or $\pi$. In the case of a vanishing interference term ($P_{\mathrm{BD}} = 0$), this phase depends only on the sign of $(P_{\mathrm{D}} - P_{\mathrm{B}})$. If the ionisation probability from the bright state is larger, the ion signal exhibits its first maximum when the wavepacket is entirely in the bright state ($\varphi_{\mathrm{B},p} = 2p\pi$). Conversely if the ionisation probability is larger from the dark state a first maximum appears after half a period of oscillation ($\varphi_{\mathrm{D},p} = (2p+1)\pi$). In the stationary basis set the

initial phase is only related to the relative signs of the dipole moments of the transitions involved. Conversely, in the bright-dark state formalism, as explained above, direct physical meaning is given to the initial phase $\varphi_0$.

The above treatment has assumed that the laser pulses are short compared to the period of the time evolution. This excludes in particular the use of chirped pulses which could "shape" the wavepacket and lead to phases that differ from the two values cited above. Extension to more than two excited states leads to new features, including the appearance of several frequencies in the oscillation pattern and the possibility of having different oscillation phase values. This situation is encountered, for example, with Rydberg states or vibrational wavepackets.

### 2.3 Application to the potassium 4p doublet states

In this section, we apply the preceding general theoretical framework to probe the dynamics in the fine structure levels in the practical case of potassium atoms excited on the $4s$–$4p$ transition. Observing fine structure dynamics with the pump-probe technique is not necessarily straightforward. One difficulty arises from the propensity rule which favours $J \rightarrow J+1$ transitions, increasing the difference between the dominant pump-probe path ($J \rightarrow J+1 \rightarrow J+2$) and the minor ones. This effect can reduce the contrast of the pump-probe oscillations, and is particularly pronounced if multiphoton transitions are involved [27]. Moreover fine structure energies are in general of a few tens of wavenumbers and coherent excitation of the fine structure levels needs subpicosecond pulses. In our case the two fine structure levels $P_{1/2}$ and $P_{3/2}$ are splitted by 57.7 cm$^{-1}$ [26] and are coherently excited by a first ultrashort pulse. These stationary states are eigenstates of the coupled basis set $|(L,S)J,M_J\rangle$, $|a\rangle = |(1,1/2)3/2,1/2\rangle$ and $|b\rangle = |(1,1/2)1/2,1/2\rangle$. Both of these states are accessible from the ground state, $|g\rangle = |(0,1/2)1/2,1/2\rangle$. Here, for the sake of simplicity, we have chosen to restrict our discussion to the case $M_J = 1/2$, although the state with the opposite value $M_J = -1/2$ exhibits equivalent behaviour. An evaluation of the 3-$j$ factors gives $\tan\alpha = \mu_{bg}/\mu_{ag} = -1/\sqrt{2}$.

In the uncoupled basis set $|L,M_L;S,M_S\rangle$, the ground state corresponding to $M_J = 1/2$ is the $|g\rangle = |0,0;1/2,1/2\rangle$ state. In this basis set, the electric dipole transition selection rules require the conservation of the spin projection $M_S$ during the transition ($\Delta M_S = 0$). For linear polarisation ($\Delta M_L = 0$) and taking the quantization axis along the polarisation vector, the bright and dark states are the eigenstates of the uncoupled basis set, $|\psi_B\rangle = |1,0;1/2,1/2\rangle$ and $|\psi_D\rangle = |1,1;1/2,-1/2\rangle$ respectively. These states have opposite orientation of the spin angular momentum. Therefore the bright state-dark state oscillation corresponds to a spin flip accompanied by a change in the direction of the orbital momentum. These states are coupled by the spin-orbit Hamiltonian which dictates the free evolution of the system. This corresponds exactly to the classical precession of both orbital (**L**) and spin (**S**) momentum around the total angular momentum (**J**) (Fig. 2). Once more, the bright state-dark state formalism provides a simple image of the dynamics of the system.

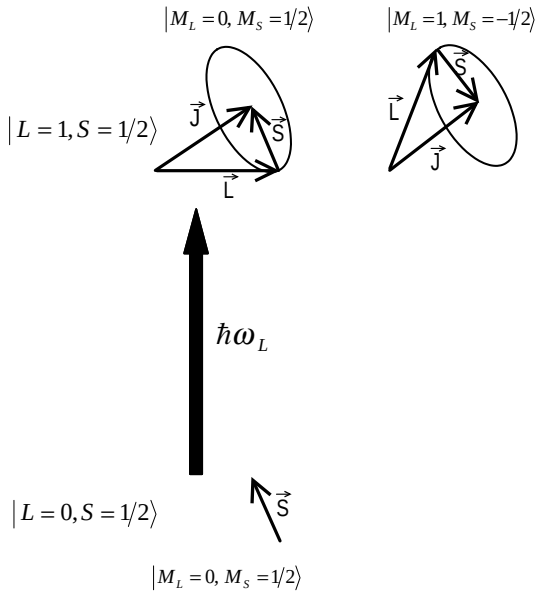


**Fig. 2.** Angular momentum in the bright state-dark state basis set: bright state $|L=1,M_L=0;S=1/2,M_S=1/2\rangle$ (left); dark state $|L=1,M_L=1;S=1/2,M_S=-1/2\rangle$ (right).

The one-photon ionisation probe leads to a superposition of photoelectrons states of kinetic energy, $E_k$, for which angular momenta can be again described in the coupled or uncoupled basis set. Although either choice is acceptable, it is most convenient to use the same basis set for the ionisation continuum as for the excited states, that is $|E_k;L^+,M_L^+;S^+,M_S^+\rangle$. We consider only the case of linear and parallel pump and probe polarisations. The electric dipole selection rules imply that the bright state can be ionised towards the $|E_k,L^+,0;1/2,1/2\rangle$ states with $L^+ = 0$ and 2, while the dark state is connected to the $|E_k,2,1;1/2,-1/2\rangle$ state only (Fig. 3a). Since the bright and dark states have no final ion states in common, the interference term in equation (7) vanishes ($P_{BD} = 0$). The relevant ionisation dipole moments are given in Table 1, together with the ionisation probabilities. The radial part (taken from numerical calculations [41]), have been interpolated at the average experimental electron energy ($E_k \cong 0.56$ eV). Since $P_B/P_D = 1.97$, the observation of the spin orbit precession is possible. An ionisation probability higher for the bright state leads to a maximum signal at $\tau = 0$ and for multiples of the oscillation period ($\varphi = 2p\pi$). Here the bright-dark state formalism provides a direct insight into the position of these maxima.

Equivalent conclusions can also be derived in the stationary representation $\{|(L,S)J,M_J\rangle\}$ with the help of equation (3). In this framework, three final states are accessible in the continuum, namely the $^2S_{1/2}$ and $^2D_{3/2}$ states which can be excited from both the $4p\ ^2P_{1/2}$ and $4p\ ^2P_{3/2}$ states and the $^2D_{5/2}$ state which can only be reached from the $4p\ ^2P_{3/2}$ state. These transitions are

**Table 1.** Ionisation dipole moments for the bright and dark states (in atomic units). Radial integrals taken from reference [41] at an electron kinetic energy $E_k \cong 0.56$ eV.

| states in the continuum | bright state ($^2$P, $M_L = 0, M_S = 1/2$) | dark state ($^2$P, $M_L = 1, M_S = -1/2$) |
|---|---|---|
| $E_k$, $^2$S $M_L = 0, M_S = 1/2$ | 2.20 | 0 |
| $E_k$, $^2$D $M_L = 0, M_S = 1/2$ | 3.18 | 0 |
| $E_k$, $^2$D $M_L = 1, M_S = -1/2$ | 0 | 2.76 |
| relative ionisation probability | 1.97 | 1 |

**Table 2.** Ionisation dipole moments and ionisation probabilities ($P_f(\tau)$) for the stationary states (coupled basis set) in atomic units. Radial integrals taken from reference [41] at a kinetic energy $E_k \cong 0.56$ eV for $M_J = 1/2$.

| final state $\|f\rangle$ | $\mu_{f^2P_{1/2}}$ | $\mu_{f^2P_{3/2}}$ | $P_f(\tau = 0)/\|\mathcal{E}_1\|^2\|\mathcal{E}_2\|^2$ (arb. units) | $P_f(\tau = \pi/\omega_{ba})/\|\mathcal{E}_1\|^2\|\mathcal{E}_2\|^2$ (arb. units) |
|---|---|---|---|---|
| $E_k$, $^2S_{1/2}$ | −1.27 | +1.80 | 14.6 | 1.6 |
| $E_k$, $^2D_{3/2}$ | −2.90 | +0.41 | 12.1 | 5.4 |
| $E_k$, $^2D_{5/2}$ | 0 | 3.02 | 18.2 | 18.2 |
| total | | | 44.9 | 25.2 |

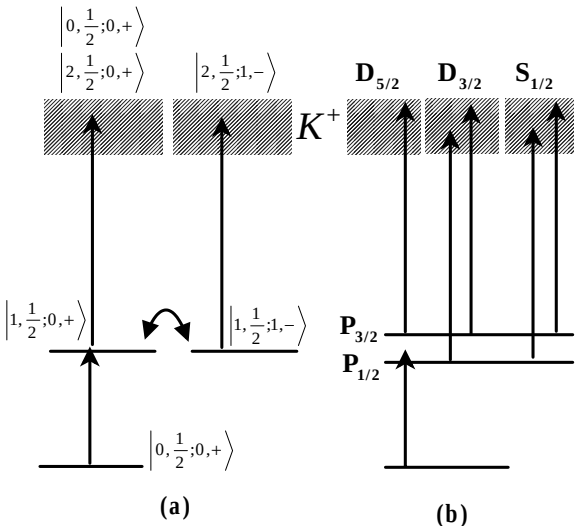


**Fig. 3.** Ionisation scheme: (a) in the uncoupled basis set and (b) in the coupled basis set.

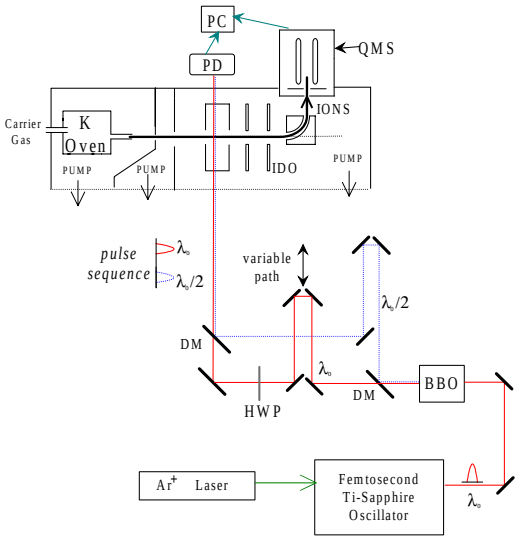


**Fig. 4.** Schematic diagram of the experimental set-up. DM: dichroic mirror; QMS: quadrupole mass spectrometer; HWP: half wave plate; IDO: ion deviation optic; PD: photodiode.

displayed in Figure 3b and the corresponding dipole moments derived from calculations of the radial wave function [41] are shown in Table 2. The ionisation probability is maximum for the highest $J$ state transition.

Quantum beats arise only when the two fine structure levels can be excited to the same final state. This is the case for the $^2S_{1/2}$ and $^2D_{3/2}$ states. The $^2S_{1/2}$ state contribution has the highest contrast since both quantum paths have equivalent weights. The sign of the dipole moment product being positive for all these transitions, the ionisation probability should be highest for delay time multiples of the oscillation period. This result is in agreement with the conclusion obtained in the bright state-dark state framework.

## 3 Experiment

### 3.1 Set-up

The experimental set-up is identical to the one used in previous experiments [34]. Briefly, it consists of a home built Ti:sapphire oscillator (750–850 nm range), an optical set-up to create the sequence of two time delayed pulses, an atomic beam of potassium seeded in helium and a quadrupole mass spectrometer Balzers QMG 421 to detect $K^+$ ion (Fig. 4). The laser was operated at $\lambda = 769$ nm with a bandwidth of $\Delta\lambda = 9$ nm, 300 mW average power and a 76 MHz repetition rate. After frequency doubling in a 1 mm thick BBO crystal, 0.3 nJ/pulse of blue radiation

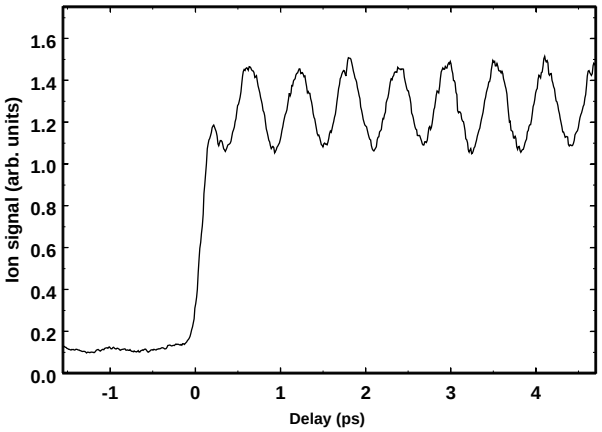


**Fig. 5.** Pump-probe results in the potassium $4p$ manifold (average of several scans). The oscillations period (580 fs) corresponds to the fine structure splitting of the $4p$ state. For negative time delays the blue pulse comes first, so that there should be no pump-probe signal. The phase of the oscillation is as predicted by the calculations of the dipole moments described in the text.

at 384.5 nm was obtained and used as the probe pulse. The remaining red radiation (20 nJ/pulse), extracted by a dichroic mirror, was used as the pump pulse. A delay ($\tau$) between the pulses was introduced by using a translating pair of mirrors placed in the infrared beam path. The two beams were then recombined and focused onto the atomic beam. The potassium oven was heated to 480 °C. The number of potassium ions was recorded as a function of the time delay between the two pulses. Taking into account the $4p$ state lifetime ($\tau_{\rm rad}$ = 27 ns [26]) and the high laser repetition rate ($T_{\rm rep}$ = 13 ns), particular attention was taken to reduce the transit time $\tau_{\rm trans}$ of the potassium atoms through the laser beams in order to eliminate contributions from pump-probe pairs separated by a multiple of $T_{\rm rep}$. Such contributions also oscillate as a function of the delay time. However the initial phase of these oscillations has no particular relationship with the phase of those observed for positive delay. This extra contribution is present at both negative and positive time delay and its average total weight is $(\mathrm{e}^{\Gamma T_{\rm rep}}-1)^{-1}$ (where $\Gamma = \tau_{\rm rad}^{-1} + \tau_{\rm trans}^{-1}$ is the effective decay rate). To drastically reduce this effect, helium was used as a carrier gas to increase the speed of the potassium beam and hence shorten the interaction time with the laser. The interaction time was further decreased by more tightly focusing the lasers onto the atomic beam. The blue (probe) laser beam was also slightly translated upstream with respect to the red (pump) one to further reduce the transit time to an effective value of the order of 7 ns.

### 3.2 Results and discussion

The results are presented in Figure 5. Several scans were recorded over the delay time range [−2 ps; +5 ps] and averaged. We observe oscillations with a period of 580 fs in agreement with the 57.7 $\mathrm{cm}^{-1}$ [26] value for the energy splitting of the fine structure doublet. The first maximum occurs at 580 fs, after one period, in agreement with the calculation of the dipole moments that leads to a higher ionisation probability when the wavepacket is in the bright state. The observed signal at negative time delays results from three contributions:

(i) the remaining oscillatory pump-probe term, mentioned in the previous section, associated with delays that are multiples of $T_{\rm rep}$ = 13 ns (0.1 times the average signal for positive delay times);
(ii) resonance-enhanced three photon ionisation from the red pulse (measured to be 70 counts/s);
(iii) non-resonant two photon ionisation; from the blue pulse (estimated to be less than 2 counts/s).

The negative delay signal is weakly modulated as a result of the first contribution. The contrast of this remaining oscillation is attenuated by the hyperfine structure in the excited state (58 MHz for the $^2\mathrm{P}_{1/2}$ state and a total of about 36 MHz for the $^2\mathrm{P}_{3/2}$ state [42]) which results in more complex wavepacket evolution than the simple scheme described above, and in the mixing of contributions of the wavepackets excited from the two ground state hyperfine levels (split by 461 MHz [42]).

In the limit of ultrashort pulses (compared to the oscillatory period), one should observe a sharp increase of the signal at time zero, followed by the free evolution which starts from a maximum and oscillates, following a cosine function. A signal resulting from the product of a cosine function with a Heavyside function would therefore be expected. The first peak "centred" at time zero would have its negative time part suppressed, and a positive time part looking exactly as those of the following peaks. When the pulse duration cannot be neglected, the oscillation function must be convoluted with a step function whose exact shape is not always easy to calculate [43]. However, one can show that the corresponding signal around $\tau = 0$ is strongly reduced compared to the following maxima as can be seen on the experimental results.

The contrast of the oscillation,

$$C = 2\frac{P_{\rm max} - P_{\rm min}}{P_{\rm max} + P_{\rm min}} \tag{9}$$

is measured to be 0.34, smaller than the predicted value of 0.56. This difference could be due to the misalignment introduced between the laser beams in order to reduce the effective transit time. Also, due to the dispersion of the lens used to focus the beams, the focal points of the red and blue pulses were shifted by about 1 cm. The observed signal is thus the result of a complex integration over atoms having encountered different laser intensities. Therefore partial saturation (for the atoms at the centre of the laser beam) cannot be totally ruled out. This saturation would result in reduction of the contrast, but would also produce an oscillation phase shift which was not observed here.

## 4 Conclusion

We have presented in this paper a pump-probe experiment performed in the $4p$ manifold of potassium atoms. A pair of femtosecond pulses have been used to excite the system and to probe it *via* photoionisation after its free evolution. The ion signal reveals the dynamics in the excited states. We have described two theoretical descriptions of the phenomena both equivalent but which provide different physical insights. More precisely, we have demonstrated how the bright-dark states formalism is the most appropriate to describe this dynamics by identifying the wavepacket as both an orbital and spin angular momentum wavepacket. Its dynamics corresponds to the precession of the orbital and spin momentum around the total angular momentum vector. This formalism could be used in order to investigate the spin polarisation of the electrons, a process that is currently under consideration.

We sincerely acknowledge Jacques Vigué for stimulating discussions and Mai Dinh for her participation in an early stage of the experiment. Mireille Aymar is particularly acknowledged for helpful discussions about the photoionisation cross-sections and communication of reference [41]. This work has been financially supported by the Centre National de la Recherche Scientifique (CNRS), the Ministère de l'Éducation Nationale, de l'Enseignement Supérieur et de la Recherche (MENESR), the Région Midi-Pyrénées and l'Institut Universitaire de France. E.S. acknowledges financial support from the Ministère des Affaires Étrangères.

## References

1. A.H. Zewail, J. Phys. Chem. **97**, 12427 (1993).
2. J. Manz, L. Wöste, *Femtosecond Chemistry* (VCH, Weinheim, New York, 1995), p. 916.
3. M. Chergui, *Femtochemistry: Ultrafast chemical and physical processes in molecular systems* (World Scientific, Singapore, 1996).
4. M.H.M. Janssen, R.M. Bowman, A.H. Zewail, Chem. Phys. Lett. **172**, 99 (1990).
5. T. Baumert, M. Grosser, R. Thalweiser, G. Gerber, Phys. Rev. Lett. **67**, 3753 (1991).
6. S. Rutz, E. Schreiber, Real-time vibrational dynamics of $K_2$, in *Ultrafast Phenomena IX*, edited by P.F. Barbara *et al.* (Springer Verlag, Berlin, 1994), Vol. 60, p. 312.
7. M.J.J. Vrakking, I. Fisher, D.M. Villeneuve, A. Stolow, J. Chem. Phys. **103**, 4538 (1995).
8. A. Assion, M. Geisler, J. Helbing, V. Seyfried, T. Baumert, Phys. Rev. A **54**, 4605R (1996).
9. S. Rutz, S. Greschik, E. Schreiber, L. Wöste, Chem. Phys. Lett. **257**, 365 (1996).
10. I. Fisher, M.J.J. Vrakking, D.M. Villeneuve, A. Stolow, Chem. Phys. **207**, 331 (1996).
11. G. Grégoire, M. Mons, I. Dimicoli, F. Piuzzi, E. Charron, C. Dedonder-Lardeux, C. Jouvet, S. Martrenchard, D. Solgadi, A. Suzor-Weiner, Eur. Phys. J. D **1**, 187 (1998).
12. C. Nicole, M.A. Bouchene, C. Meier, S. Magnier, E. Schreiber, B. Girard, J. Chem. Phys. **111**, 7857 (1999).
13. M. Dantus, M.J. Rosker, A.H. Zewail, J. Chem. Phys. **87**, 2395 (1987).
14. T.S. Rose, M.J. Rosker, A.H. Zewail, J. Chem. Phys. **88**, 6672 (1988).
15. M.J. Rosker, M. Dantus, A.H. Zewail, J. Chem. Phys. **89**, 6128 (1988).
16. T. Baumert, B. Bühler, R. Thalweiser, G. Gerber, Phys. Rev. Lett. **64**, 733 (1990).
17. M.J.J. Vrakking, D.M. Villeneuve, A. Stolow, J. Chem. Phys. **105**, 5647 (1996).
18. J.A. Yeazell, C.R. Stroud Jr, Phys. Rev. Lett. **60**, 1494 (1988).
19. A. ten Wolde, L.D. Noordam, A. Lagendijk, H.B. van Linden van den Heuvell, Phys. Rev. Lett. **61**, 2099 (1988).
20. M. Strehle, U. Weichmann, G. Gerber, Phys. Rev. A **58**, 450 (1998).
21. J.A. Ramswell, V.G. Stavros, J. Lei, Q. Hong, H.H. Fielding, Phys. Rev. A **59**, 2186 (1999).
22. R. van Leeuwen, M.L. Bajema, R.R. Jones, Phys. Rev. Lett. **82**, 2852 (1999).
23. J.F. Christian, L.C. Snoek, S.G. Clement, W.J. van der Zande, Phys. Rev. A **53**, 1894 (1996).
24. C. Nicole, M.A. Bouchene, S. Zamith, N. Melikechi, B. Girard, Phys. Rev. A **60**, R1755 (1999).
25. S. Haroche, Quantum beats and time-resolved fluorescence spectroscopy, in *High-resolution laser spectroscopy*, edited by K. Shimoda (Springer-Verlag, Berlin, 1976), Vol. 13, p. 256.
26. A.A. Radzig, B.M. Smirnov, *Reference Data on Atoms, Molecules, and Ions* (Springer, Berlin, 1985).
27. V. Blanchet, C. Nicole, M.A. Bouchene, B. Girard, Phys. Rev. Lett. **78**, 2716 (1997).
28. M.A. Bouchene, V. Blanchet, C. Nicole, N. Melikechi, B. Girard, H. Ruppe, S. Rutz, E. Schreiber, L. Wöste, Eur. Phys. J. D **2**, 131 (1998).
29. R.R. Jones, D.W. Schumacher, T.F. Gallagher, P.H. Bucksbaum, J. Phys. B **28**, L405 (1995).
30. L.C. Snoek, S.G. Clement, F.J.M. Harren, W.J. van der Zande, Chem. Phys. Lett. **258**, 460 (1996).
31. R.R. Jones, C.S. Raman, D.W. Schumacher, P.H. Bucksbaum, Phys. Rev. Lett. **71**, 2575 (1993).
32. R.R. Jones, C.S. Raman, D.W. Schumacher, P.H. Bucksbaum, Femtosecond Ramsey fringes in strongly-driven Rydberg systems, in *AIP Conference Proceedings* (AIP, 1993), Vol. 290, p. 319.
33. M. Bellini, A. Bartoli, T.W. Hansch, Opt. Lett. **22**, 540 (1997).
34. V. Blanchet, M.A. Bouchene, B. Girard, J. Chem. Phys. **108**, 4862 (1998).
35. S. Mukamel, *Principles of Nonlinear Optical Spectroscopy* (Oxford University Press, New York, 1995).
36. E. Arimondo, *Coherent population trapping in laser spectroscopy*, edited by E. Wolf (Elsevier, Amsterdam, 1996), Vol. 35, p. 257.
37. A. Aspect, E. Arimondo, R. Kaiser, N. Vansteenkiste, C. Cohen-Tannoudji, Phys. Rev. Lett. **61**, 826 (1988).
38. U. Gaubatz, P. Rudecki, S. Schiemann, K. Bergmann, J. Chem. Phys. **92**, 5363 (1990).
39. K. Bergmann, H. Theuer, B.W. Shore, Rev. Mod. Phys. **70**, 1003 (1998).
40. N.V. Vitanov, J. Phys. B **31**, 709 (1998).
41. S.T. Wane, Thèse d'état, Paris-Sud, 1988.
42. E. Arimondo, M. Inguscio, P. Violino, Rev. Mod. Phys. **49**, 31 (1977).
43. B. De Beauvoir, V. Blanchet, M.A. Bouchene, B. Girard (in preparation).